Объединенный институт ядерных исследований

# RELATIVISTIC NUCLEAR PHYSICS: from HUNDREDS of MeV to TeV

## 9th International Workshop

*Modra-Harmonia, Slovakia, May 22–27, 2006*
*Proceedings of the Workshop*

# РЕЛЯТИВИСТСКАЯ ЯДЕРНАЯ ФИЗИКА: от СОТЕН МэВ до ТэВ

## 9-е международное совещание

*Модра-Гармония, Словакия, 22–27 мая 2006 г.*
*Труды совещания*

Дубна 2006

# QCD MATTER: A SEARCH FOR A MIXED QUARK-HADRON PHASE

A.N. Sissakian[a], A.S. Sorin[a,1] and V.D. Toneev[a]

*a) JINR, 141980, Dubna, Moscow region, Russia*

**Abstract**

Physics aspects of a JINR project to reach the planned 5A GeV energy for the Au and U beams and to increase the bombarding energy up to 10A GeV are discussed. The project aims to search for a possible formation of a strongly interacting mixed quark-hadron phase. The relevant problems are exemplified. A need for scanning heavy-ion interactions in bombarding energy, collision centrality and isospin asymmetry is emphasized.

## 1. Introduction

Over the last 25 years a lot of efforts have been made to search for new states of strongly interacting matter under extreme conditions of high temperature and/or baryon density, as predicted by Quantum Chromodynamics (QCD). These states are relevant to understanding the evolution of the early Universe after Big Bang, the formation of neutron stars, and the physics of heavy-ion collisions. The latter is of great importance since it opens a way to reproduce these extreme conditions in the Earth laboratory. This explains a permanent trend of leading world research centers to construct new heavy ion accelerators for even higher colliding energy.

Looking at the list of heavy-ion accelerators one can see that after the pioneering experiments at the Dubna Synchrophasotron, heavy-ion physics developed successfully at Bevalac (Berkley) with the bombarding energy to $E_{lab} \sim$ 2A GeV, AGS (Brookhaven) $E_{lab} \sim$ 11A GeV, and SPS (CERN) $E_{lab} \sim$ 160A GeV. The first two machines are closed now. The nuclear physics programs at SPS as well as at SIS (GSI, Darmstadt, $E_{lab} \sim$ 1A GeV) are practically completed. The new relativistic heavy-ion collider (RHIC, Brookhaven) is intensively working in the ultrarelativistic energy range $\sqrt{s_{NN}} \sim 200$ GeV to search for signals of the quark-gluon plasma formation. In this respect, many hopes are related to the Large Hadron Collider (LHC, CERN) which will start to operate in the TeV region in two-three years. The low-energy scanning program at SPS (NA49 Collaboration) revealed an interesting structure in the energy dependence of some observables at $E_{lab} \sim 20 - 30$A GeV which can be associated with the exit of an excited system into a deconfinement state. This fact essentially stimulates a new large project FAIR GSI (Darmstadt) for studying compressed baryonic matter in a large energy range of $E_{lab} = 10 - 30$A GeV which should come into operation after 2015 year [1]. These problems are so attractive that the RHIC scientific society discusses a possibility to decrease the collider energy till the FAIR range [2].

On the other hand, in JINR there is a modern superconducting accelerator, Nuclotron, which has not realized its planned parameters yet. The Veksler and Baldin Laboratory of High Energy has certain experimental facilities and large experience in working with heavy ions. This study may actively be supported by theoretical investigations of the Bogoliubov Laboratory of Theoretical Physics. In [3] a program

[1]E-mail: sorin@theor.jinr.ru

was proposed for investigating the dense strongly interacting QCD matter, formed in relativistic heavy ion collisions, based on acceleration of heavy ions like Au at the Nuclotron up to the maximal planned energy $E_{lab}$ = 5A GeV. In view of new opened opportunities of the Nuclotron update to increase the bombarding energy up to 10A GeV and to get both Au and U ions with relativistic energies, the relevant physics problems are discussed in this paper.

## 2. Phase diagrams

A convenient way to present a variety of possible states of strongly interacting matter is a phase diagram in terms of temperature $T$ and baryon chemical potential $\mu_B$ (or baryon density $\rho_B$), as presented in Fig.1. This picture shows in which region of the diagram the given phase is realized and which colliding energies are needed to populate this region.

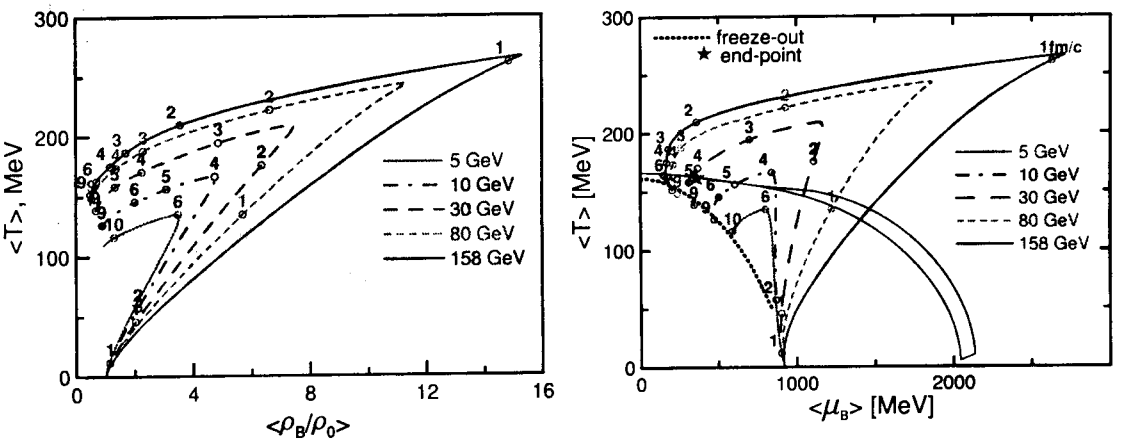


Figure 1: Dynamical trajectories for central ($b$ = 2 fm) Au+Au collisions in $T-\rho_B$ (left panel) and $T-\mu_B$ (right panel) plane for various bombarding energies calculated within the relativistic 3-fluid hydrodynamics calculated with hadronic EoS [4]. Numbers near the trajectories are the evolution time moment. Phase boundaries are estimated in a two-phase bag model [5]. In the right panel the critical end-point calculated in the lattice QCD [6] is marked by the star and the shaded region corresponds to uncertainties of the bag model.

As is seen, a system, formed in a high energy collision, is fast heated and compressed and then starts to expand slowly reaching the freeze-out point which defines observable hadron quantities. At the Nuclotron energy $E_{lab}$ = 5A GeV the system "looks" into the mixed phase for a short time (the left part of Fig.1), however, uncertainties of these calculations are still large. To get agreement with the lattice data for finite $T$ and $\mu_B$, masses of $u, d$ quarks should be rather heavy, and the phase boundary is shifted towards higher $\mu_B$ [5] (the right part in Fig.1). On the other hand, one should exercise caution because these dynamical trajectories were calculated for a pure hadronic gas equation of state, and the presence of a phase transition may noticeably change them. In addition, near the phase transition the strongly interacting QCD system behaves like a liquid rather than a gas, as was clarified recently at small $\mu_B$ from both quark [7] and hadronic [8] side. As to high $\mu_B$ values, it is a completely open question. One should also note that as follows from lattice QCD calculations for $\mu_B \approx 0$ the deconfinement temperature practically coincides with the transition temperature for chiral symmetry

restoration while for baryon-rich matter it is still an open question.

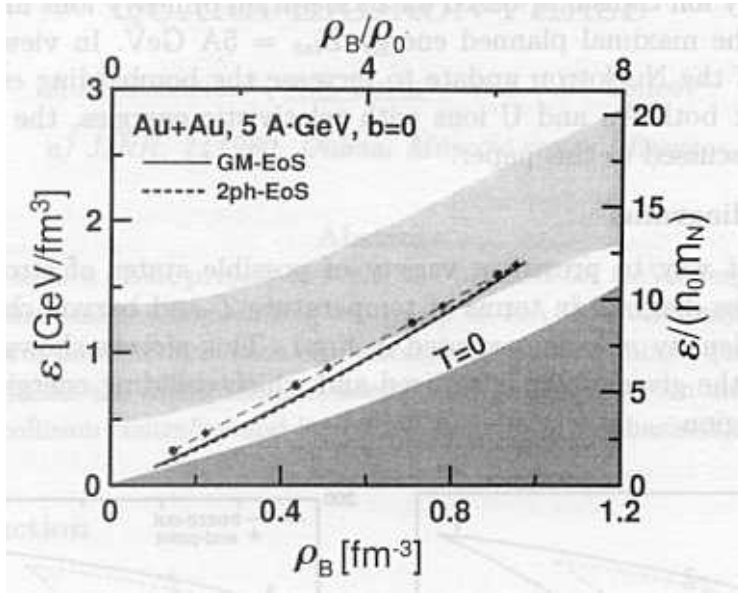


Figure 2: Dynamical trajectory in the $\varepsilon - \rho_B$-plane for central Au+Au collisions calculated with two equations of state: pure hadronic (solid line) and with first order phase transition (dashed). Spatial averaging is done over the cube with the 4 fm sides and Lorentz contracted in the longitudinal direction [9]. The shaded regions correspond to the mixed phase (upper one) and the non-reachable domain with the boundary condition $T = 0$, respectively.

In Fig.2, dynamical trajectories in the $\varepsilon - \rho_B$ plane for the top project Nuclotron energy are given for two equations of state, without and with the first-order phase transition [4, 9]. The shaded band corresponds to the mixed phase of more restrictive EoS with heavy masses of $u, d$ quarks, as shown in the right panel of Fig.1. Nevertheless, both the trajectories, being close to each other, spend some time in the mixed phase. The main difference between the results presented in Fig.1 and Fig.2 comes from the different averaging procedures used: in the first case, thermodynamic quantities were averaged over the whole volume of the interacting system, while in the second case, it was carried out only over a cube of 4 fm sides placed at the origin being Lorentz contracted along the colliding axis. Thus, for central collisions at the 5A GeV Nuclotron energy even if an average state of the whole strongly interacting system does not approach the mixed phase, an essential part of the system volume will spend a certain time in this mixed phase. An experimental consequence is that an expected observable signal of reaching the mixed phase should be rather weak. Note that for $E_{lab}$ =10A GeV these conditions for a phase transition are fulfilled appreciably better.

One should stress that the presented above dynamical trajectories and boundaries for the first-order phase transition were estimated for a system conserving a single charge, namely the baryonic charge. However, the behavior of this system near the phase transition and particularly within the mixed phase will be qualitatively different if conservation of more than one charge is taken into account [10, 11]. So we turn to consideration of effects of additional conservation of the electric charge, or isospin of the system.

We shall characterize the charge asymmetry by the electric-to-baryonic charge ratio $Z/A = \rho_Q/\rho_B$ or by the isospin ratio $x = (\rho_Q - \rho_B)/2\rho_B$ which are related as $x =$

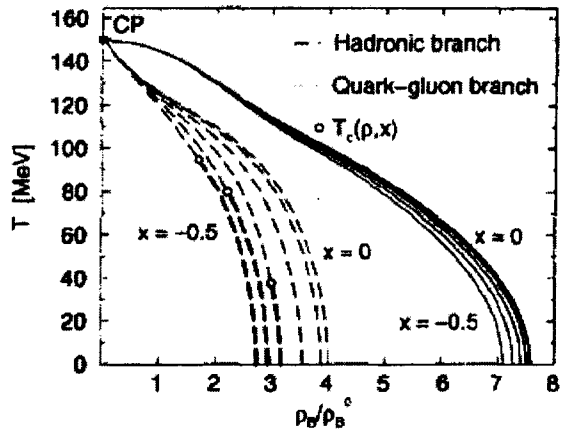


Figure 3: Projections of the boundary surface on the $(\rho_B, T)$ plane at different $x$. The isospin ratios are $x = 0, -0.1, -0.2, -0.3, -0.4, -0.5$, starting from the right. The boundaries of the mixed phase with the quark and hadron phase are plotted as solid and dashed lines, respectively [12].

$Z/A - 0.5$. For Au+Au collisions we have $Z/A = 0.4$ or $x = -0.1$.

An essential difference in the first-order phase transition for systems with one and two conserved charges stems from the fact that the phase boundary, which is a line for a single charge conservation, is getting a two-dimensional surface. In the latter case the conserved charges can now be shared by two phases in equilibrium in different concentration in each phase but consistent with the global charge conservation. If this is energetically favored by the internal forces and Fermi energies, then these degrees of freedom will be exploited by the system and will influence thermodynamic quantities.

The boundary surface, so called binodal, may be parameterized in a different way, say as $\{T, \mu_B, \mu_Q\}$, $\{T, \mu_B, x\}$, $\{T, \rho_B, x\}$ or $\{p, \rho_B, x\}$. In Fig.3, some $\{T, \rho_B, x\}$ projections of a hadron-quark phase transition are shown [12].

It is seen that, for example, in symmetric matter at $T = 0$ the baryon density ranges along $3.5\rho_0$ between the onset and completion of the transition. For $x = 0$ the hadron boundary is close to that in the left panel of Fig.1. This mixed phase domain becomes even larger in density for iso-asymmetric systems. Another important observation is that the density at the onset (i.e. hadronic side of the phase boundary at the transition density $\rho_c$) decreases with increasing isospin asymmetry. If one compares points for $x = 0$ and $x = -0.2$ at $T = 0$, a decrease is $\delta\rho_B \approx 0.5\rho_0$. But this effect is practically absent for $T \gtrsim 120$ MeV.

A more realistic description of the hadronic phase, which takes into account the density dependence of hadron masses and coupling constants [14], was used for the results presented in Fig.4. The general trend of curves is quite similar to that in Fig.3 but now the values of transition densities are higher though the same bag constant $B^{1/4}$ =187 MeV was used in both the calculations [12, 14]. The main difference comes from the very low mass used for in-medium nucleon at the normal nuclear density and $T = 0$, $M_N^* = 0.6M_N$. In this case the coefficient $C_4$ ahead the highest sigma-meson interaction term $C_4\sigma^4$ turns out to be negative and, therefore, such a system should be unstable [14]. If the bag constant increases, the transition boundary moves to higher values. Note that in both the cases the temperature $T(\mu_B = 0)$ is lower than the value 170-180 MeV expected from the lattice calculations. However, the lattice QCD

data show that we deal with the first-order phase transition only for the high baryon chemical potential, above that for the critical end-point [6] (see also the right panel in Fig.1). Thus, it is not completely clear whether two-phase calculations should describe the lattice value of $T(\mu_B = 0)$. Appropriate lattice QCD data are available only for small $\mu_B$ and there are no data taking into consideration the conservation of both baryon and electric charges.

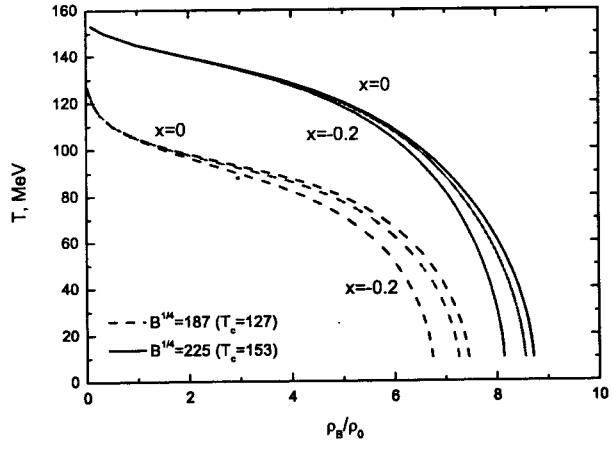


Figure 4: Hadron boundary of the mixed phase at different $x$ [13]. The isospin ratios are $x = 0, -0.1, -0.2$, starting from the right. Hadronic phase is described within the relativistic mean-field approach with density-dependent hadron masses and coupling constants [14]. The results are given for two values of the bag constant: $B^{1/4}$ =187 (dashed lines) and 225 MeV (solid lines).

Even noticeably stronger reduction of the transition density with increasing neutron fraction is predicted by the Catania group [15] for $T = 0$. It was demonstrated that $\rho_c$ depends appreciably on poorly known properties of EoS at high baryon densities. This statement is illustrated in Fig.5. Note quite low values of the transition densities which originate from small values of the bag constant used, $B^{1/4} = 140 - 170$ MeV. This choice is argued by the following Witten hypothesis [18]: a state made of an approximately equal number of $u, d, s$ quarks can have the energy per baryon number smaller than that for Fe; therefore, the quark matter is absolutely stable and purely quark stars may exist. This hypothesis put strong constraints on quark model parameters: The bag model parameter $B$ should be small [18]. Today the existence of pure quark stars is not excluded but is rather considered as an exotic case. In this respect, the (non)observation of a strong isospin dependence of the transition density may be treated as a test of the Witten hypothesis.

The most striking feature of all results is a sharp decrease of the transition density $\rho_c$ which takes place in the range $Z/A \sim 0.3 \div 0.45$, though the size of the reduction effect and its position on the $Z/A$ axis, as is seen in Fig.5, are strongly model dependent. Nevertheless, application of neutron-rich heavy ions seems to be very perspective to study the mixed QCD matter at energies even lower than the project Nuclotron energy 5A GeV. Dynamical trajectories presented in Fig.5 show that the phase boundary may be reached at energies as low as 1A GeV.

As follows from Figs.3-5, the most favorable temperatures for this reduction effect are in the range $T \lesssim 80$ MeV. It is well known that in central collisions of relativistic

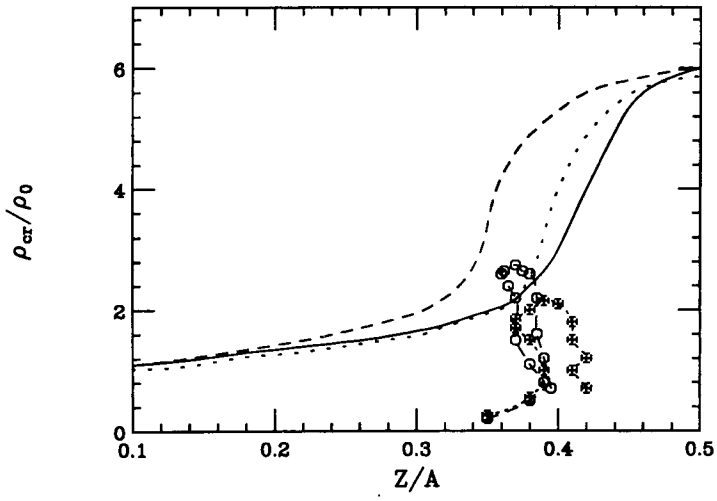


Figure 5: Variation of the transition density with the proton fraction at $T = 0$ for various EoS parameterizations of the relativistic mean-field theory: Dotted, dashed and solid lines correspond to the GM3 version [16], to an additional inclusion of non-linearity in $\rho$ interaction [17] and to an extra term describing the interaction of the isovector $\delta$-meson [15], respectively. The points represent the dynamical trajectory in interaction zone during semi-central $^{132}Sn$ + $^{132}Sn$ collisions at 1A GeV (circles) and at 300A MeV (crosses) [15].

heavy ions the growth of the density $\rho_B > 3\rho_0$ with the energy increase is accompanied by the appropriate rise in temperature $T \gtrsim 100$ MeV. Available stable nuclei cover only a very narrow region in isospin asymmetry $Z/A \approx 0.39 \div 0.40$ exhausted by the $^{238}_{92}U$ and $^{197}_{79}Au$ isotopes, respectively, what embarrasses checking the boundary reduction effect. The use of the long-lived $^{195}_{79}Au$ isotope ($\tau_l$ ~150 days) allows one to move towards neutron-poor side of the boundary till $Z/A$ =0.41. In addition, the construction of accelerators of intense beams of neutron-rich heavy ions with $Z/A$ beyond this narrow region is an extremely complex technological problem. [15]. Some possibility to get lower temperatures and to extend the reached isospin asymmetry region is opened by study of semi-central rather than central collisions. This possibility is illustrated in Fig.6

It is noteworthy that after about 10 fm/$c$ the quadruple momentum is almost vanishing and a nice local equilibration is achieved. At this beam energy the maximum density coincides with reaching the thermalization. Then the system is quickly cooling while expanding. In Fig.6 one can see that rather exotic nuclear matter is formed in a transient time of the order of 10 fm/$c$, having the baryon density around $3\rho_0$, the temperature $50 - 60$ $MeV$, the energy density 500 $MeV$ fm$^{-3}$ and the proton fraction between 0.35 and 0.40. So the local neutron excess well inside the estimated mixed phase region may be even higher than that in colliding nuclei (note that for $^{238}U$ the isospin symmetry ratio is $Z/A$ =0.387).

The $\{p, \rho_B, x\}$ projections of EoS corresponding to the Maxwell construction are given in Fig.7 for two isotherms. In accordance with the result familiar from the behavior of the systems with one conserved charge, for symmetric matter ($x = 0$) the pressure stays constant within the mixed phase. In contrast, at $x < 0$ the pressure changes during the transition increasing with the baryon density. This change of the pressure throughout the phase separation in asymmetric systems is an indication of

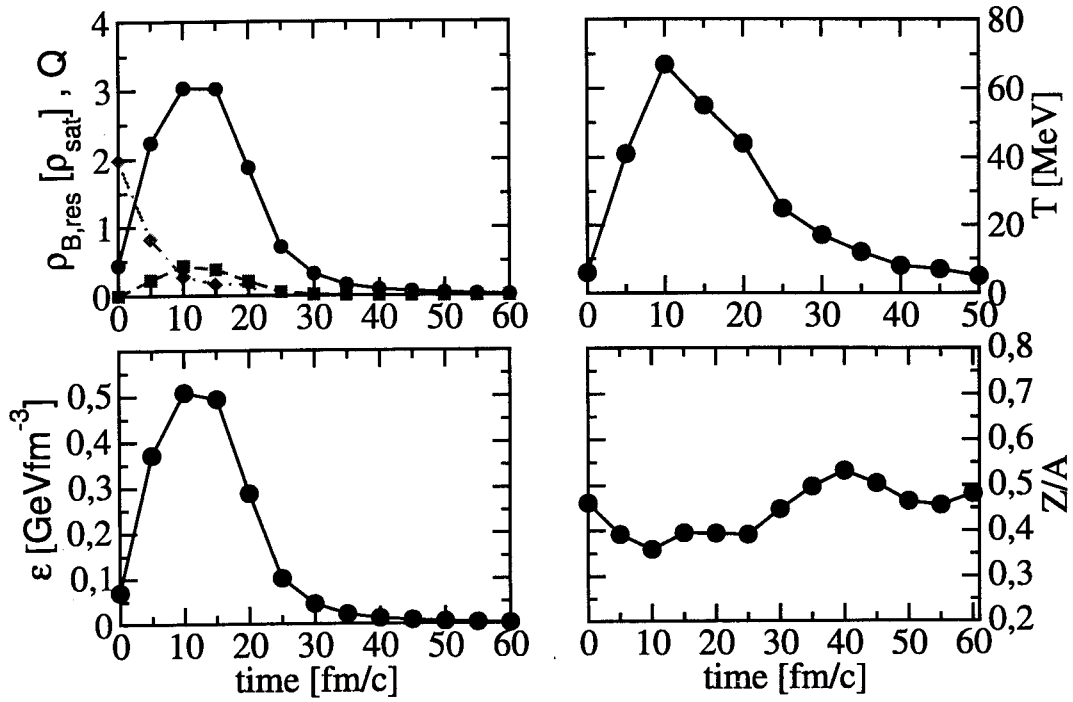


Figure 6: Time evolution of thermodynamic quantities inside a cubic cell of 2.5 fm wide, located in the center of mass of the system, is shown for semi-central $^{238}U$ $-^{238}U$ collisions at $E_{lab}$ =1A GeV with $b$ =7 fm. Baryon density, temperature, energy density and proton fraction are presented. Different curves in the upper-left panel are: *black dots* – the baryon density in $\rho_0$ units; *grey dots* – the quadruple momentum in momentum space; *squares* – the resonance density [15].

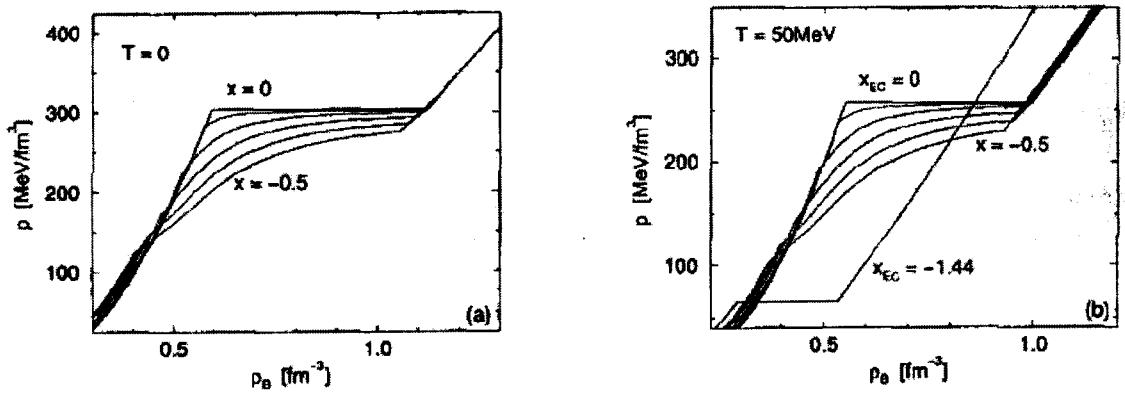


Figure 7: Isoterms for different values of $x$ at $T = 0$ (left panel) and $T = 50$ MeV (right panel). The isospin ratios are $x = 0, -0.1, -0.2, -0.3, -0.4, -0.5$ from top to bottom [12].

a smoother transition than in symmetric systems as was first noted in the context of neutron star calculations [11]. Certainly, such behavior of pressure may crucially affect the evolution of two colliding nuclei.

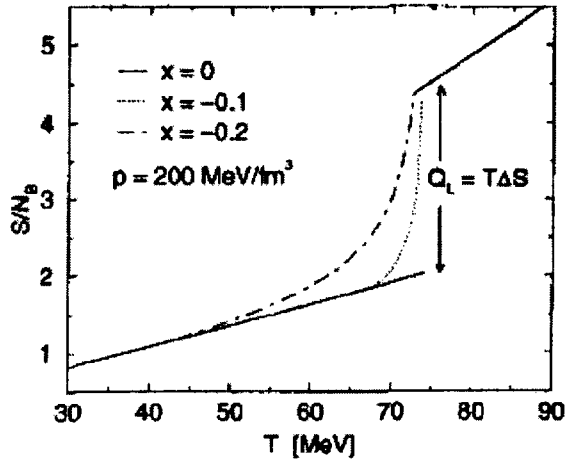


Figure 8: Entropy per baryon as a function of temperature at the constant pressure for various isospin ratios [12]. For the case $x = 0$ the latent heat $Q_L$ is shown.

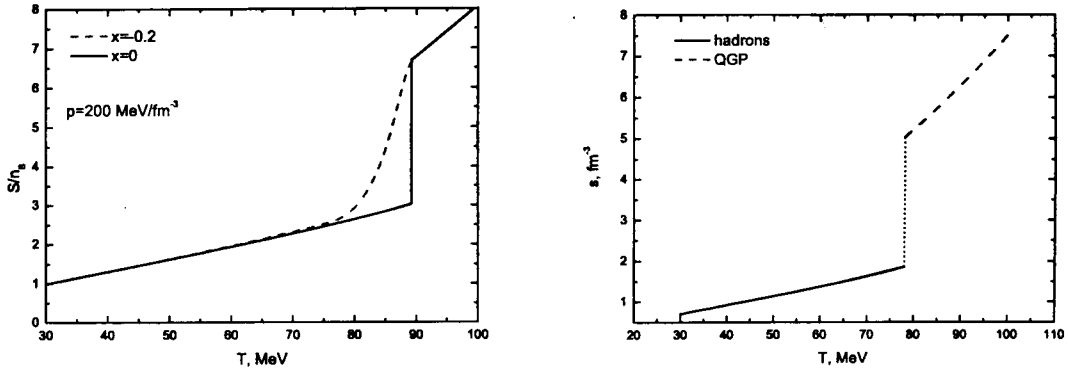


Figure 9: Entropy per baryon as a function of temperature at the constant pressure for various isospin ratios (left panel) and entropy as a function of temperature at the constant chemical potentials $\mu_B$ =1300, $\mu_S$ =300 and $\mu_Q$ =-100 MeV (right panel). The relativistic mean-field model with the density-dependent interaction is used for the hadronic phase and the bag model describes the quark phase [13].

Along with pressure, the temperature as well as the baryonic and electric chemical potentials do not remain constant within the mixed phase. This behavior is responsible for disappearance of the entropy discontinuity at the given $p$ and $x$ as pictured in the right panel of Fig.8. This fact gave grounds for author [12] to claim that in the iso-asymmetric matter the first-order phase transition is smoothed and becomes the second-order phase transition. One should note that in spite of such behavior of the entropy, the first derivative of the thermodynamic potential with respect to temperature at the constant chemical potentials (i.e. locally in the $\mu_i$ space) suffers a

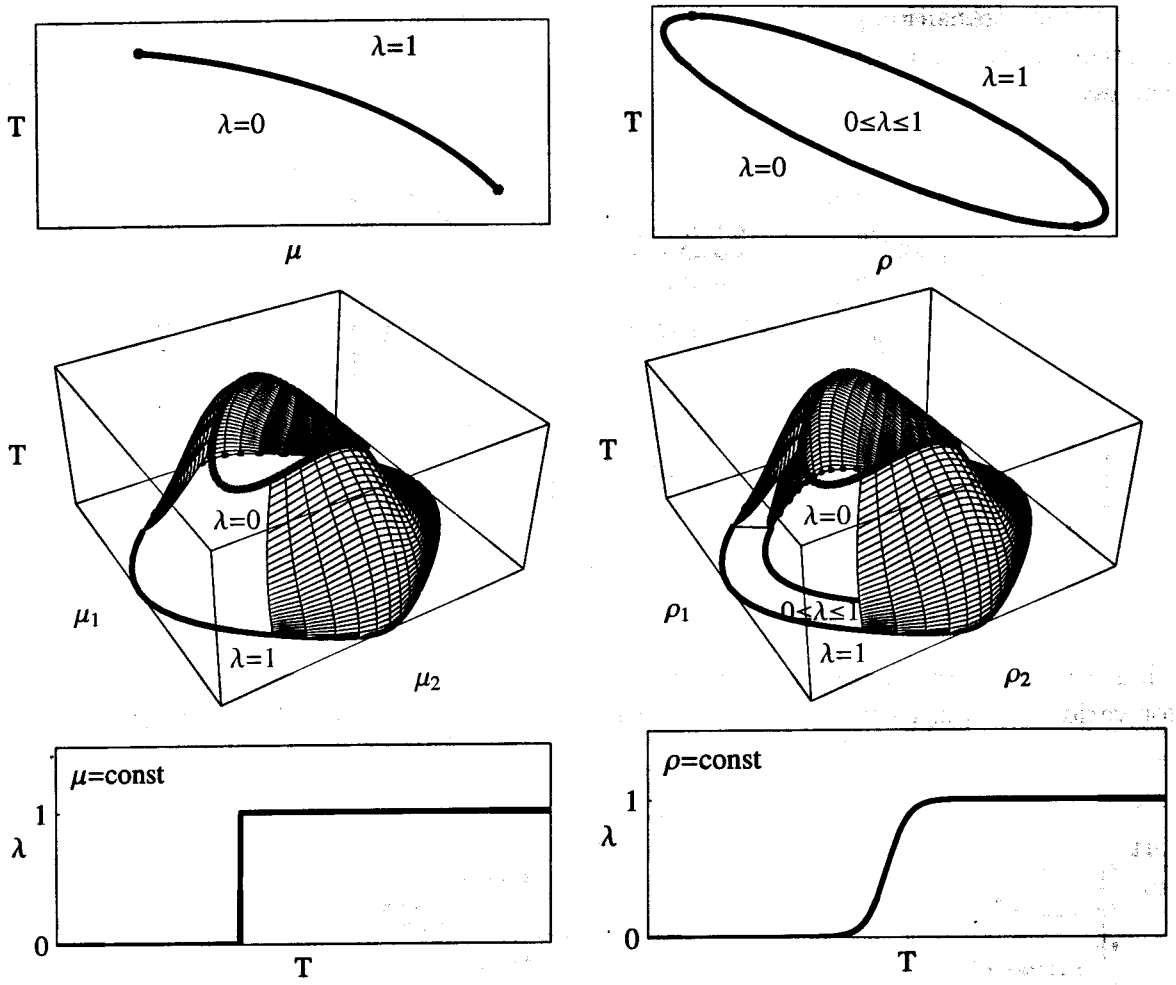


Figure 10: Schematics view on the mixed phase boundaries in the $\{T, \mu\}$ (on left) and $\{T, \rho\}$ (on right) representations. Boundaries for a system conservation of a single charge (top), two charges (middle) as well as the volume fraction (bottom) are presented [19].

jump (see Fig.9), what is evidence of the first-order phase transition in iso-asymmetric matter. At the same time if the $\{p, \rho_B, x\}$ representation of entropy is used, the result of [12] is well reproduced (see the left panel of Fig.8). This mirrors a general property inherent to systems with the first-order phase transition: In the mixed phase the first derivatives of the thermodynamic potential have discontinuity in the $\{T, \mu_1, ..., \mu_n\}$ representation but they are continuous in the $\{T, \rho_1, ..., \rho_n\}$ one. That is the direct consequence of the Gibbs phase-equilibrium conditions [10] from which follows that in the first representation the every point of the $n$-dimensional mixed phase surface maps unambiguously on the $\{T, \mu_1, ..., \mu_n\}$ space. Evidently, it is not the case in the $\{T, \rho_1, ..., \rho_n\}$ representation [19] as illustrated in Fig.10. Due to that the volume fraction of the second phase $\lambda \equiv \frac{V_{II}}{V}$ jumps when the system enters in the mixed phase, if the first representation is used, while it does not in the second representation. Any extensive thermodynamic quantity $A$ will follow this behavior of $\lambda$ since $A = \lambda A_{II} + (1 - \lambda) A_I$.

As was noted above, the presence of two conserving charges in the $\{T, \mu_B, \mu_Q\}$ representation changes dimensionality of the two-phase coexistence surface for the first-order

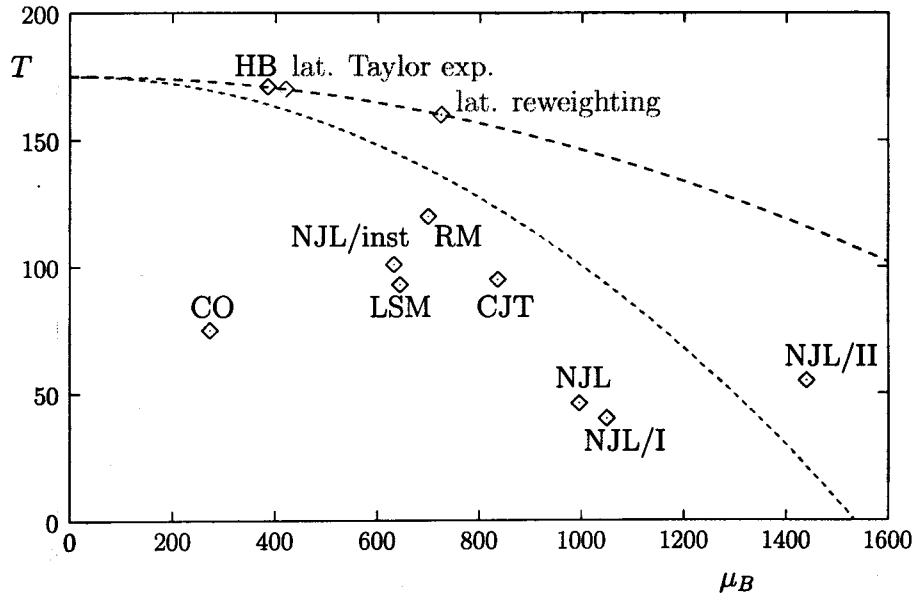


Figure 11: Theoretical (model and lattice) predictions for the location of the critical end-point. Two lines are obtained by lattice Taylor expansion where the lower curve corresponds to smaller quark masses (compare with Fig.1). Points are calculated in different models specified in [20]. Errors/uncertainities are not shown.

phase transition. Namely, the one-dimensional line for the case of a single conserving charge transforms into a two-dimensional (or $n$-dimensional) (hyper)surface if two (or $n$) charges are conserved [10], see Fig.10. Therefore, the manifold of critical points, that by definition is the boundary of the mixed phase where the system suffers the second order phase transition, also changes sufficiently: From two isolated points defining the limited line of the mixed phase it transforms into a one-dimensional curve ($(n-1)$-dimensional (hyper)surface) being a boundary of two-dimensional ($n$-dimensional) coexistence (hyper)surface [19]. The different topologies of the mixed phase states may result in different important consequences. In particular, in the discussed now new projects of FAIR [1] and RHIC [2] aimed to search for manifestation of the critical end-point, being the point where the first-order phase transition of the QCD matter ends, it may turn out that it is not a point but hypersurface those dimensionality is defined by a number and properties of conserving charges [19]. It is noteworthy that the location of the critical end-point in the $T-\mu_B$ plane was estimated in both various model and lattice QCD calculations, however, without taking into account isospin asymmetry degree of freedom. But even in this case the predictions vary wildly as demonstrated in Fig.11 taken from [20].

The outstanding problems involved in understanding the hadron-quark matter phase transition, aside from the description of these phases themselves, are related to the geometric structure of the mixed phase and its evolution with varying the relative fraction $\lambda$ of phases. If one of the conserved charges is the electric charge, a geometric structure in the mixed phase is expected. The nucleation mechanism for cluster formation (say, quark drops in the hadron environment) is dominant in the metastable region of the first-order phase transition and formation of the mixed phase influenced by finite size effects due to nonvanishing surface tension at the interface between the hadronic and quark matter and the Coulomb energy of the formed drops.

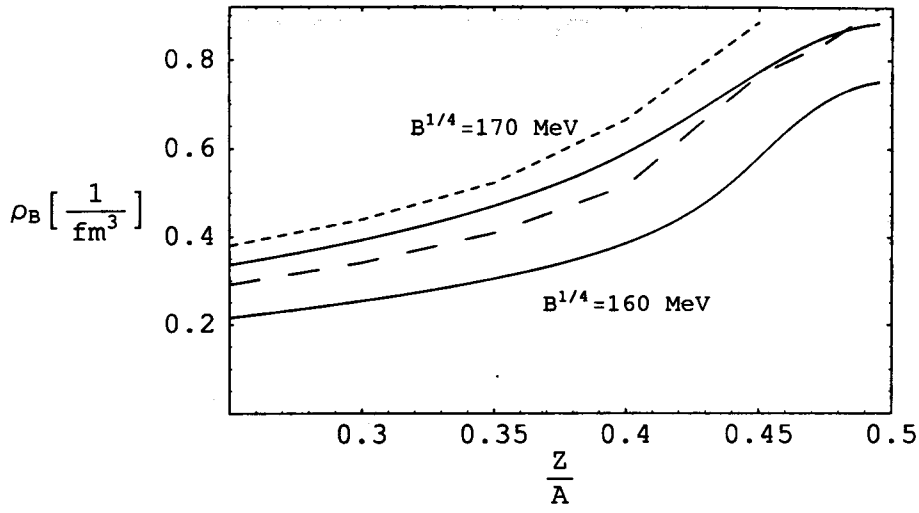


Figure 12: Transition density as a function of $Z/A$ at $T = 50$ MeV [15]. The solid lines are obtained neglecting finite-size effects. The results plotted as long and short-dashed lines take into account these effects and correspond to $B^{1/4} = 160$ MeV and $B^{1/4} = 170$ MeV, respectively.

The geometric structure of the mixed phase was studied in some detail for neutron star matter (see the review-article [21]) but for nuclear matter uncertainties are rather large. In Fig.12, an estimate of the finite-size effects is presented for the nuclear case [15].

As is clearly seen, the value of the density at which the mixed phase can be reached becomes larger, if the finite size effects are taken into consideration. This increase due to finite-size effects is larger for smaller values of the bag constant $B$ (compare with results in Fig.4). Nevertheless, a strong dependence of the transition energy on $Z/A$ survives even in this case [15].

Besides the isospin there is yet another nuclear parameter which may influence evolution of a colliding system. It is the nuclear shape. It was noted earlier [22, 23] that deformation and orientation affect compression, elliptic flow and particle production for collisions of Uranium nuclei. As seen from Fig.13, the compression in the tip-tip U+U collisions is about 30% higher and the region with $\rho > 5\rho_0$ lasts approximately 40% longer than in the body-body collisions or spherical U+U collisions. Moreover, the nucleon elliptic flow has some unique features which in principle may allow one to disentangle these two orientations [2]. Such situation is valid for the energy range 1-20A GeV [22] but uncertainties are still large [23].

### 3. On signals and precursors

Similarly to the general situation with searching for a quark-gluon plasma in ultra-relativistic collisions, there is no single crucial experiment which unambiguously solves the problem. It is quite evident that direct information on the mixed phase may be obtained only by means of weakly interacting photon and lepton probes. Sensitivity of global hadron observables to possible phase transitions is expected to be weak, but it might not be the case for more delicate characteristics. In any case, due to the proximity of the phase diagram region under discussion to the confinement transition and chiral symmetry restoration, some precursory phenomena cannot be excluded at

[2]We are thankful to N. Xu for drawing our attention to this issue.

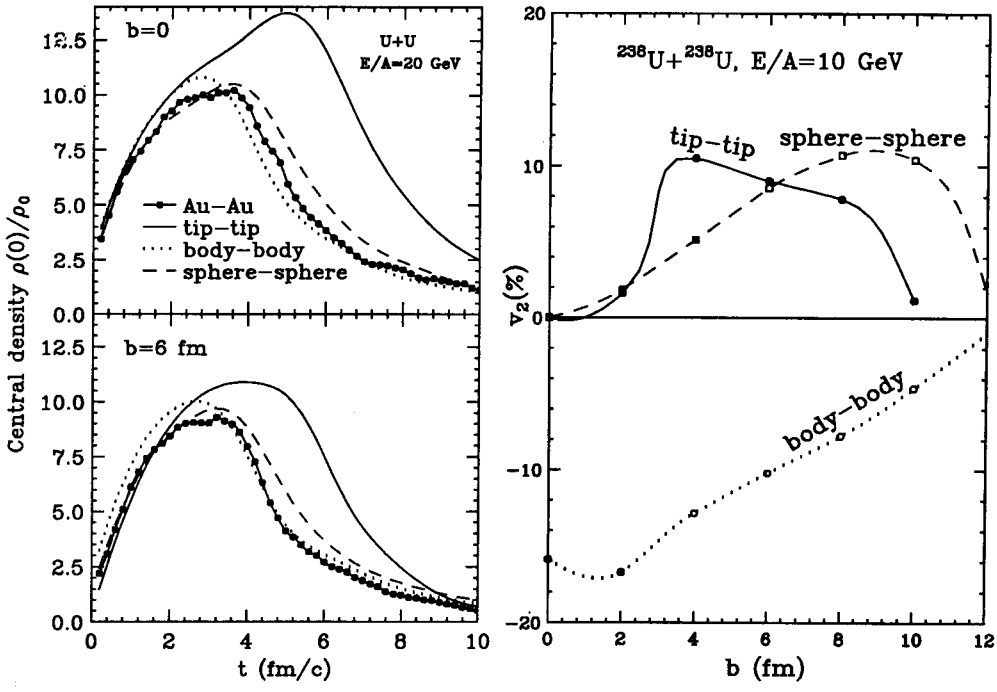


Figure 13: Evolution of central baryon density for Au+Au and U+U collisions at 20A GeV (left panel) and impact parameter dependence of nucleon elliptic flow at 10A GeV (right panel) for different orientations of deformed Uranium nuclei as well as for spherical ones [22].

the bombarding energy below 10A GeV, which opens a new perspective for physical investigations at the Dubna Nuclotron.

Properties of hadrons are expected to change in hot and/or dense baryon matter [24, 25]. This change concerns hadronic masses and widths, first of all those for the $\sigma$-meson as the chiral partner of pions which characterizes a degree of chiral symmetry violation and can serve as a "signal" of its restoration as well as the mixed phase formation. Rare decays in matter of vector mesons (particularly $\rho$ and $\omega$) are also very attractive.

Nevertheless, there are theoretical proposals to probe chiral symmetry restoration in the vicinity of the phase transition boundary. In particular, it was shown [26, 27] that a two-photon decay of the $\sigma$-meson formed as an intermediate state in $\pi\pi$ scattering may be a very attractive signal. As depicted in Fig.14, at temperature in the vicinity of the phase transition, when $m_\sigma \sim 2m_\pi$, there is an anomalous peak in invariant mass spectra of $\gamma$ pairs which may serve as a signal of the phase transition and formation of a mixed phase. Certainly, there is a huge combinatorial background due to $\pi^0 \to \gamma\gamma$ decays, but the Nuclotron energy is expected to have some advantage against higher energy accelerators because the contribution of gamma's from deconfined quarks-gluons will be negligible.

To measure this signal, a photon spectrometer is needed. The installation of this kind, two-arm $\gamma$-spectrometer PHOTON-2, is available at JINR. The ability of this installation in discriminating two correlated photons is demonstrated in Fig.15.

The presented invariant mass spectrum of $\gamma\gamma$ correlations is based on $1.5 \cdot 10^6$ selected dC-interactions. A peak corresponding to about 5000 $\eta$-meson decays is clearly seen at $M_\eta = 540.5 \pm 2.1$ MeV with the resolution $\sigma = 33.4 \pm 6.0$ [28]. The measured $\eta$ mass is consistent with the table value. A huge peak from the $\pi^0 \to \gamma\gamma$ decay is strongly

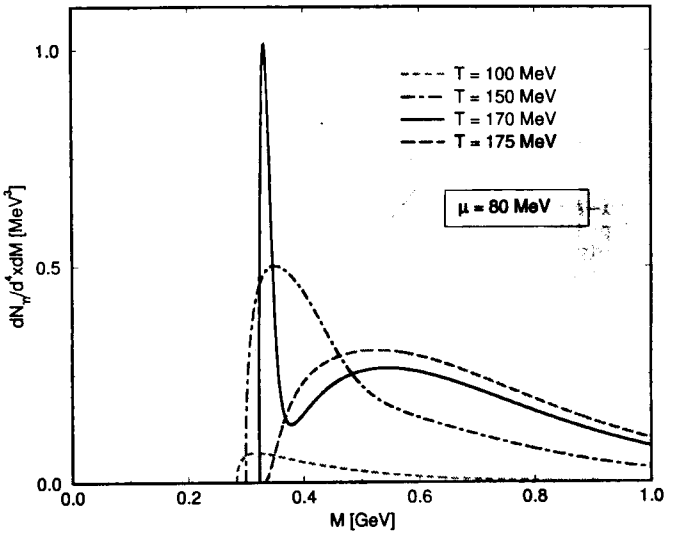


Figure 14: Invariant mass spectra of $2\gamma$ at $\mu_B = 80$ MeV and different temperatures [27].

suppressed here and is not visible in the figure due to the selection criteria of events to increase the signal/background ratio. It is of interest that some additional structure with a maximum in the range of 340-460 MeV is seen which was not observed in analogous experiments with lower statistics [28]. The nature of this resonance structure is under discussion now.

Fluctuations in particle number are inherent in the first-order phase transition and formation of a metastable mixed phase. However, to a certain extent, peculiarities of a phase transition will be washed out by transition dynamics and subsequent hadron interactions which drive the system closer to equilibrium, which means the loss of information on the system prehistory. Nevertheless, it was understood that the study of fluctuations in relativistic strongly interacting matter may help with solving the problems mentioned above. Experimental data on event-by-event fluctuations (e.g., fluctuations in particle multiplicity, electric, baryon and strangeness charges) in nuclear collisions give a unique possibility to test recent ideas on the origin of fluctuations in relativistic interacting systems [29, 30]. Among them the suppression of event-by-event fluctuations of electric charge was predicted [29] as a consequence of deconfinement. Theoretical estimates of the magnitude of the charge fluctuations indicate that they are much smaller in a quark-gluon plasma than in a hadron gas. Thus, naively, a decrease in the fluctuations is expected when the collision energy crosses the threshold for the deconfinement phase transition. However, this prediction is derived under assumptions that initial fluctuations survive through hadronization and that their relaxation times in hadronic matter are significantly longer than in the hadronic stage of the collision [29, 31].

More realistic estimates have been done recently for the hadron resonance-gas model within a statistical approach [32]. The equilibrium statistical model was successfully used to describe the data on hadron multiplicities in relativistic heavy-ion collisions [33]. The system was treated in Grand Canonical (GCE) and Canonical (CE) Ensembles with taking into account the conservation of baryon, electric and strangeness charges. The decay of resonances was included in fluctuations which were calculated for nuclear

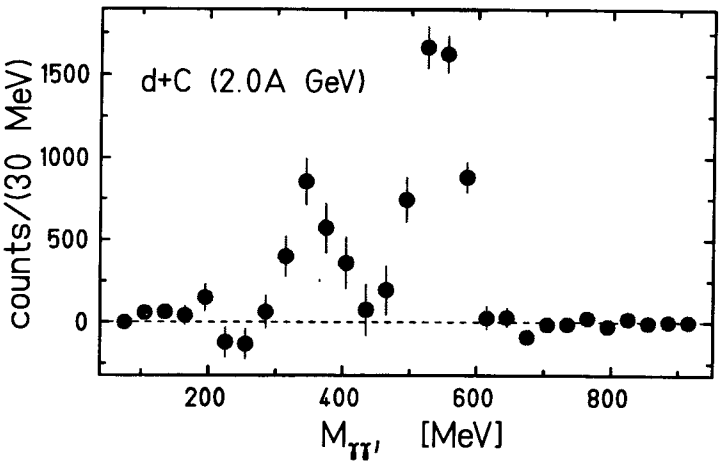


Figure 15: Invariant mass distribution of pairs of $\gamma$ quanta with the energy $E_\gamma > 100$ MeV after subtraction of the combinatorial background in the $d + C \rightarrow \gamma + \gamma + X$ reaction at the bombarding energy 2A GeV [28].

states to be realized along the experimental freeze-out curve. The whole available energy range, from SIS to RHIC energies, was covered in this study [32].

We exemplify these predictions by the results in Fig.16 for the scaled variance of negatively and positively charged hadrons,

$$\omega^- = < (\Delta N^-)^2 > / < N^- > \quad \text{and} \quad \omega^+ = < (\Delta N^+)^2 > / < N^+ > \ ,$$

where $N^\pm$ is the number of particles in the given event and $< ... >$ denote averaging over all events.

As is seen from the comparison of the GCE and CE results in Fig.16, the exact charge conservation is very important in the Nuclotron energy. While the energy $E_{lab} \sim$ 10A GeV is approached, the resonance decay is getting sizable. There is essentially different behavior of the scaled variances for negative, $\omega^-$, and positive, $\omega^+$, charges in the Nuclotron energy range $E_{lab} \lesssim 10$A GeV [32].

At a first glimpse, these statistical results may serve as a reference point to look for peculiarities related to a possible formation of the mixed phase. However, it is not the case due to at least two reasons. First, in addition to the considered statistical fluctuations, heavy-ion collisions generate dynamical fluctuations. Secondly, the above presented results correspond to an ideal situation when all final hadrons are accepted by the detector. Indeed, as was shown in [34] with using a transport approach to heavy-ion collisions, the fluctuations in the initial energy deposed in the statistical system yield dynamical fluctuations of all macroscopic parameters. In its turn, these fluctuations are dominated by a geometric variation of the impact parameter. However, even for the fixed impact parameter a number of participants fluctuates from event to event. The centrality of the selected events is commonly controlled by a number of measured projectile spectators. It was noted in [34] that this procedure introduces some asymmetry between fluctuations in target and projectile, thereby the scaled variances $\omega^-$ and $\omega^+$ behave differently in the target and projectile rapidity regions. Thus, the above noted first and second reasons are turned out to be closely related. A first attempt to compare these results with the NA49 data at $E_{lab} = 158$A GeV shows a remarkable disagreement but unfortunately it is still impossible to make any conclusions

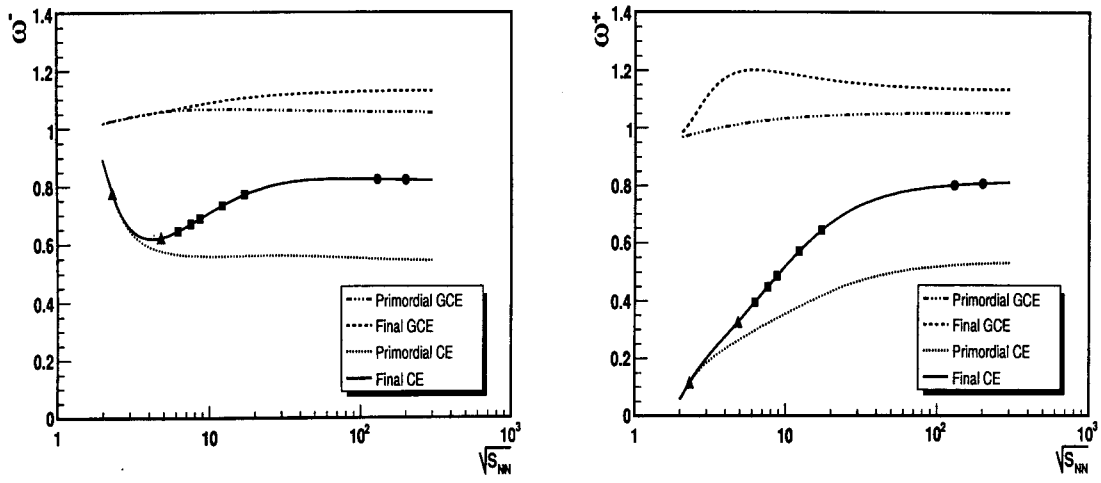


Figure 16: The colliding energy dependence of the scaled variances for negatively $\omega^-$ (left panel) and positively $\omega^+$ (right panel) charged particles calculated along the chemical freeze-out line for central Pb+Pb (Au+Au) collisions [32]. Different lines present primordial and final (i.e. including resonance decays) GCE and CE results. Solid points show the actual energy values of AGS (triangles), SPS (squires) and RHIC (dots) .

from this fact due to large uncertainties in these experimental data [34]. Note that the considered approaches take into account no phase transition. To search for signals of the mixed phase in fluctuations, the observable effect should be tested against its variations in bombarding energy, centrality selection and isospin asymmetry of colliding nuclei.

One should stress that measurements of fluctuations require tracking detectors of large acceptance, good particle identification and a precise control of collision centrality on event-by-event basis. Previous experiments suffered either small phase-space coverage or limited tracking and particle identification, therefore new measurements at the Nuclotron energy are of particular importance. From the experimental point of view the Nuclotron energy range seems to be ideal for these measurements. This is because moderate particle multiplicity and their relatively broad angular distribution simplify an efficient detection of all produced charged particles.

A particular property of the mixed phase is the so-called distillation effect: While the total charge is conserved, its distribution between two phases is different. The structure of the mixed phase is especially rich and complicated if the conservation of the baryon number, electric charge and strangeness are taken into consideration simultaneously. The distillation effect is expected to result in certain observable effects as discussed in [35, 36].

One should note that the use of neutron-rich isotopes or, generally, radioactive beams has recently become a central theme in nuclear and astro-physics researches. At present, there are several facilities devoted to nuclear physics studies using *low-energy* beams of radioactive species including the Spiral at Ganil (Caen, France), ACCULINNA and DRIBs (Dubna, Russia), Cyclotron Research Center (Louvain-la-Neuve, Belgium), TRIUMF (Vancouver, Canada), Holifield Radioactive Ion Beam Facility (Oak Ridge, USA). These capabilities for radioactive beams will eventually allow

for detailed studies of the structure of nuclei on the path of astrophysical $r$-process and provide for fundamental nuclear structure studies of very neutron-rich nuclei but with small atomic numbers. Heavy-ion radioactive beams are also of great interest for both nuclear structure studies and some astro-physics problems, in particular, clarification of the role of new $\nu p$-process in nucleosynthesis of nuclei with $A \sim 100$ [37]. To our knowledge, there is no project to get accelerated heavy neutron-rich nuclei. Unfortunately, heavy nuclear isotopes which can be obtained in a reasonable amount cannot really be extended beyond the region of the isospin asymmetry parameter $0.39 \lesssim Z/A \lesssim 0.41$ reachable with stable nuclei.

## 4. Conclusions

A study of the phase diagram of strongly interacting QCD matter in the domain populated by heavy-ion collisions with the bombarding energy $\lesssim$ 10A GeV and a search for manifestation of the mixed phase formation seem to be a very attractive task. The use of the isospin asymmetry as an additional conserving parameter to characterize the created hot and dense system draws new interest in this problem. Unfortunately, the available theoretical predictions are strongly model dependent giving rather dispersive results. There are no lattice QCD predictions for this highly nonpertubative region. So much theoretical work should be done and only future experiments may disentangle these models.

A JINR Nuclotron possibility of accelerating heavy ions to the project energy of 5A GeV and increasing it up to 10A GeV can be realized in about two-three years. This will enable us to effort a unique opportunity for scanning heavy-ion interactions in energy, centrality and isospin asymmetry of the system to search for the mixed phase of QCD matter. For the latter point it seems to be optimal to have the gold and uranium beams in order to scan in isospin asymmetry in both central and semi-central collisions at not so high temperatures favorable for observation of the phase boundary reduction. The use of strongly deformed U nuclei is quite promising to probe the orientation effect in heavy ion collisions. All this gives a chance to address experimentally many recent problems within the next several years before the FAIR GSI accelerator comes into operation. Being supplemented by scanning in the isospin asymmetry parameter, as discussed in the present paper, the proposed research program at the Nuclotron [3] may be considered also as a pilot study preparing for subsequent detailed investigations at SIS-100/300 [1] and as an integral part of the world scientific cooperation to study the energy dependence of hadron production properties in nuclear collisions.

## Acknowledgements

We greatly appreciate many useful and valuable discussions on physics, detectors and accelerator technique with Kh.Y. Abraamyan, J.G. Brankov, Yu.P. Gangrsky, M. Gazdzicki, M.I. Gorenstein, G.G. Gulbikyan, H. Gutbrod, T. Hollman, Yu.B.Ivanov, M.G. Itkis, A.S. Khvorostukhin, A.D. Kovalenko, R. Lednicky, A.I. Malakhov, I.N. Meshkov, Yu.E. Penionzhkevich, V.B. Priezzhev, V.N. Russkikh, Yu.M. Sinyukov, V.V. Skokov, M.K. Suleymanov, G.M. Ter-Akopyan, D.N. Voskresensky, N. Xu, and G.M. Zinovjev. We would like also to express our special thanks to V.G. Kadyshevsky, V.A. Matveev, and A.N. Tavkhelidze for their interest to this paper.

This work was supported in part by RFBR Grant N 05-02-17695 and by the special program of the Ministry of Education and Science of the Russian Federation (grant RNP.2.1.1.5409).

# References


[1] *Proposal for an International Accelerator Facility for Research with Heavy Ions and Antiprotons*, http://www.gsi.de/documents/DOC-2004-Mar-196-2.pdf .

[2] G.S.F. Stephans, arXiv:nucl-ex/0607030; A.Cho, Science **312**, p.190, 2006.

[3] A.N. Sissakian, A.S. Sorin, M.K. Suleymanov, V.D. Toneev, and G.M. Zinovjev, arXiv:nucl-ex/0601034; In: *Proceedings of the 8th International Workshop "Relativistic Nuclear Physics: From hundreds MeV to TeV"*, (Dubna, May 23 - 28, 2005), Dubna, 2006, p.306 [arXiv:nucl-ex/0511018].

[4] Y.B. Ivanov, V.N. Russkikh and V.D. Toneev, Phys. Rev. **C 73**, p.044904, 2006 [arXiv:nucl-th/0503088].

[5] A.S. Khvorostukhin, V.V. Skokov, V.D. Toneev and K. Redlich, arXiv:nucl-th/0605069.

[6] Z. Fodor and S.D. Katz, JHEP **203**, p.14, 2002 [arXiv:hep-lat/0106002]; JHEP **404**, p.50, 2004 [arXiv:hep-lat/0402006].

[7] E.V. Shuryak and I. Zahed, arXiv:hep-ph/0307267.

[8] D.N. Voskresensky, Nucl. Phys. A **744**, p.378, 2004 [arXiv:hep-ph/0402020]; G.E. Brown, Ch,-H. Lee, and M. Rho, arXiv:hep-ph/0402207.

[9] Yu. Ivanov, Multi-fluid hydrodynamics, Talk at the CBM Collaboration Meeting "FAIR, The physics of compressed baryonic matter", December 15-16, 2005, GSI, Darmstadt, http://www.gsi.de/documents/DOC-2005-Dec-87-112-1.pdf; V.N. Russkikh, privite communication.

[10] L.D. Landau and E.M. Lifshitz, *Statistical Physics* (Addison-Wesley, Reading, MA, 1969), Chap. VIII, IX.

[11] N.K. Glendenning, Phys. Rev. **D46**, p.1274, 1992.

[12] H.Müller, Nucl. Phys. **A 618**, p.349, 1997 [arXiv:nucl-th/9701035].

[13] A.S Khvorostukhin, V.D. Toneev and D.N. Voskresenski (to be published).

[14] E.E. Kolomeitsev and D.N. Voskresenski, Nucl. Phys. **A759**, p.373, 2005 [nucl-th/0410063].

[15] M. Di Toro, A. Drago, T. Gaitaos, V. Greco and A. Lavagno, arXiv:nucl-th/0602052.

[16] N.K. Glendenning and S.A. Moszkowski, Phys. Rev. Lett. **67**, p.2414, 1991.

[17] B. Liu, V. Creco, V. Baran, M. Colonna and M. Di Toro, Phys. Rev. **C65**, p.045201, 2002.

[18] E. Witten, Phys. Rev. **D30**, p.272, 1984.

[19] A.S Khvorostukhin, A.N. Sissakian, V.V. Skokov, A.S. Sorin, and V.D. Toneev (to be published).

[20] M. Stephanov, Int. J. Mod. Phys. **A20**, p.4387, 2005 [arXiv:hep-ph/0402115].

[21] T. Maruyama, T. Tatsumi, T. Endo and S. Chiba, arXiv:nucl-th/0605075.

[22] Bao-An Li, Phys. Rev. **C61**, p.021903, 2000 [arXiv:nucl-th/9910030].

[23] E.V. Shuryak, Phys. Rev. **C61**, p.034905, 2000 [arXiv:nucl-th/9906062]; A.J. Kuhlman and U.W. Heinz, Phys. Rev. **C72**, p.037901, 2005 [arXiv:nucl-th/0506088]; C. Nepali, G. Fai and D. Keane, Phys. Rev. **73**, p. 034911, 2006 [arXiv:hep-ph/0601030].

[24] T. Hatsuda and T. Kunihiro, Phys. Rep. **247**, p.221, 1994.

[25] G.E. Brown and M. Rho, Phys. Rep. **269**, p.333, 1996.

[26] S. Chiku and T. Hatsuda, Phys. Rev. **D58**, p.076001, 1998 [arXiv:hep-ph/9809215]; T. Hatsuda, T. Kunihiro and H. Shimizu, Phys. Rev. Lett. **82**, p.2840, 1999.

[27] M.K. Volkov, E.A. Kuraev, D. Blaschke, G. Röpke and S.M. Schmidt, Phys. Lett. **B424**, p.235, 1998 [arXiv:hep-ph/9706350].

[28] Kh.U. Abraamyan, A.N. Sissakian and A.S. Sorin, arXiv:nucl-ex/0607027.

[29] S. Jeon and V. Koch, Phys. Rev. Lett. **85**, p.2076, 2000 [arXiv:hep-ph/0003168]; M. Asakawa, U.W. Heinz and B. Muller, Phys. Rev. Lett. **85**, p.2072, 2000 [arXiv:hep-ph/0003169]; E.V. Shuryak and M.A. Stephanov, Phys. Rev. C **63**, p.064903, 2001 [arXiv:hep-ph/0010100].

[30] V.V. Begun, M. Gazdzicki, M.I. Gorenstein, and O.S. Zozulya, Phys. Rev. **C70**, p.034901, 2004 [arXiv:nucl-th/0404056]; V.V. Begun, M.I. Gorenstein, A.P. Kostyk and O.S. Zozulya, Phys. Rev. **C 71**, p.054904, 2005 [arXiv:nucl-th/0410044]; A. Keranen et al, J. Phys. **G 31**, p.S1095, 2005 [arXiv:nucl-th/0411116].

[31] J. Zaranek, Phys. Rev. C **66**, p.024905, 2002 [arXiv:hep-ph/0111228].

[32] V.V. Begun et a., arXiv:nucl-th/0606036.

[33] P. Braun-Munzinger, K. Redlich and J. Stachel, in *Quark Gluon Plasma 3* eds. R.C. Hwa and X.N. Wang, World Scientific, Singapore, p.491 [nucl-th/0304013]; A. Andronic, P. Braun-Munzinger and J. Stachel, arXiv:nucl-th/0511071.

[34] V.P. Konchakovski et al., Phys. Rev. **C73**, p.034902, 2006 [arXiv:nucl-th/0511083]; V.P. Konchakovski, M.I. Gorenstein, arXiv:nucl-th/0606047.

[35] V. Baran, M. Colonna, V. Greco and M. Di Toro, Phys. Rep. **410**, p.335, 2005.

[36] V.D. Toneev, E.G. Nikonov, B. Friman, W. Nörenberg, and K. Redlich, Eur. Phys. J. **C32**, p.99, 2004 [arXiv:hep-ph/0308088].

[37] C. Fröhlich, et al., Phys. Rev. Lett. **96**, p.142502, 2006 [arXiv:astro-ph/0511376].